Supporting Information

One-Pot Synthesis of Enhanced Dye-Sensitized Persistent Luminescence Nanoparticles to Alleviate Concentration Quenching

*Zi-Jin Wei, Kai Long, Chang Yin, Xinxin Yuan, Mengjie Sun, Wei Wang and Zhi Yuan**

Affiliations:
Key Laboratory of Functional Polymer Materials of Ministry of Education, Institute of Polymer Chemistry, College of Chemistry, Nankai University, Tianjin 300071, China.

*Corresponding author: Prof. Zhi Yuan, E-mail: zhiy@nankai.edu.cn

Contents

Table S1 ICP of metallic elements corresponding molar ratios of ZGC_n PLNPs.

Elements	$ZGC_{0.3}$ Molar Ratio (%)	$ZGC_{0.6}$ Molar Ratio (%)	$ZGC_{1.2}$ Molar Ratio (%)	$ZGC_{1.8}$ Molar Ratio (%)
Zn	35.71	36.2	35.11	36.15
Ga	64.18	63.57	64.44	63.15
Cr	0.11	0.23	0.45	0.7

The final elements molar ratios:

$ZGC_{0.3}$: Zn/Ga/Cr = 1: 1.80: 0.0031
$ZGC_{0.6}$: Zn/Ga/C = 1: 1.76: 0.0063
$ZGC_{1.2}$: Zn/Ga/Cr = 1: 1.83: 0.013
$ZGC_{1.8}$: Zn/Ga/Cr = 1: 1.75: 0.019

Table S2 ICP of metallic elements corresponding molar ratios of $ZGC_{0.6/1.2}$@OAm-RhB PLNPs.

Elements	$ZGC_{0.6}$@OAm-RhB Molar Ratio (%)	$ZGC_{1.2}$@OAm-RhB Molar Ratio (%)
Zn	36.39	36.3
Ga	63.39	63.25
Cr	0.22	0.45

The final elements molar ratios:
$ZGC_{0.6}$@OAm-RhB: Zn/Ga/C = 1: 1.74: 0.006
$ZGC_{1.2}$@OAm-RhB: Zn/Ga/Cr = 1: 1.74: 0.012

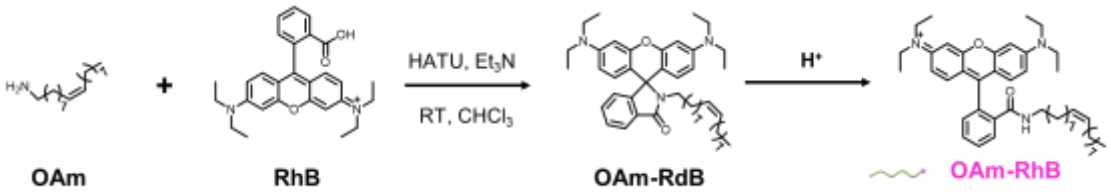

Scheme S1. The Synthesis route of OAm-RhB. Under the action of solvent OA, OAm-RdB undergoes ring-opening to form OAm-RhB.

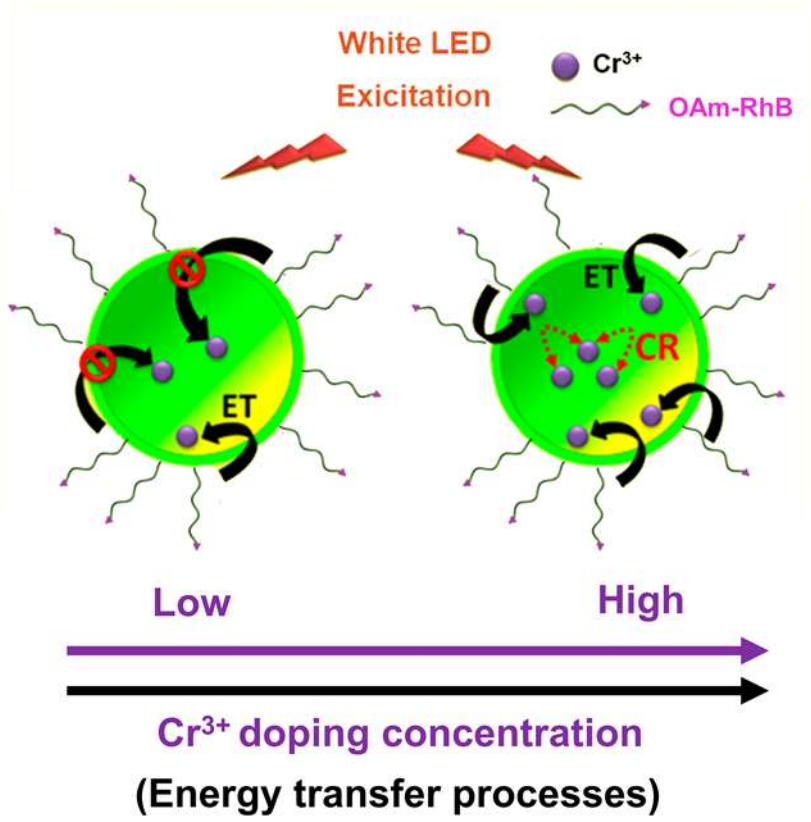

Scheme S2. The mechanism of alleviating quenching caused by high Cr^{3+} concentrations through dye sensitization (CR: cross-relaxation).

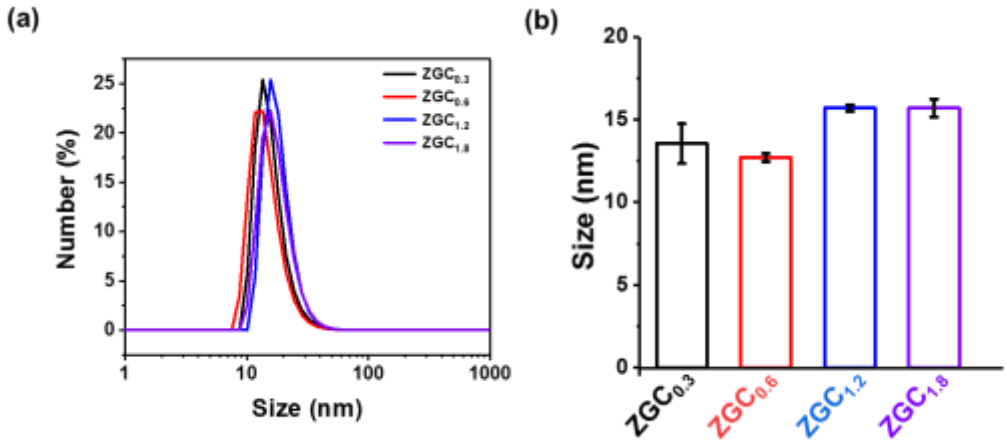

Figure S1. DLS data (a) and statistics analysis (b) of the ZGC_n PLNPs. Values were expressed as the mean ± SD (n = 3).

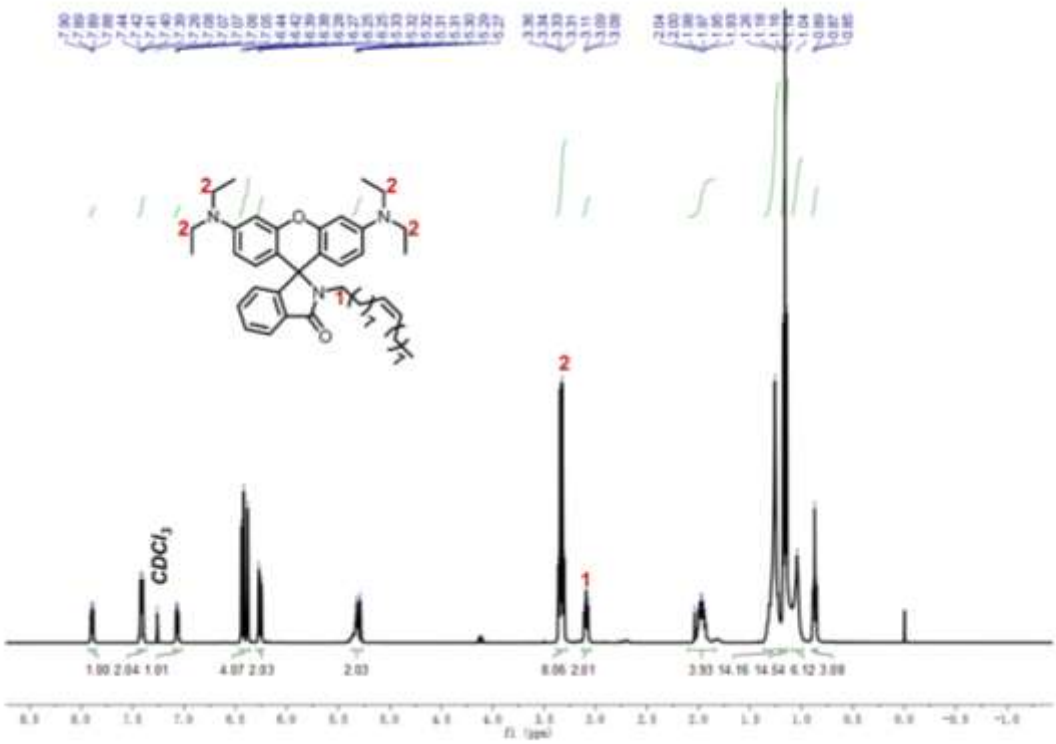

Figure S2. The ^1H NMR spectrum of OAm-RdB in $CDCl_3$.

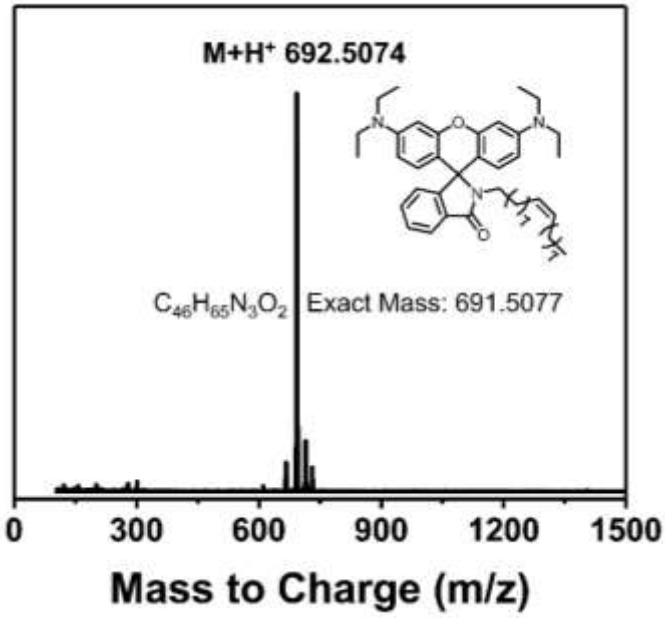

Figure S3. The ESI-MS spectrum of OAm-RdB.

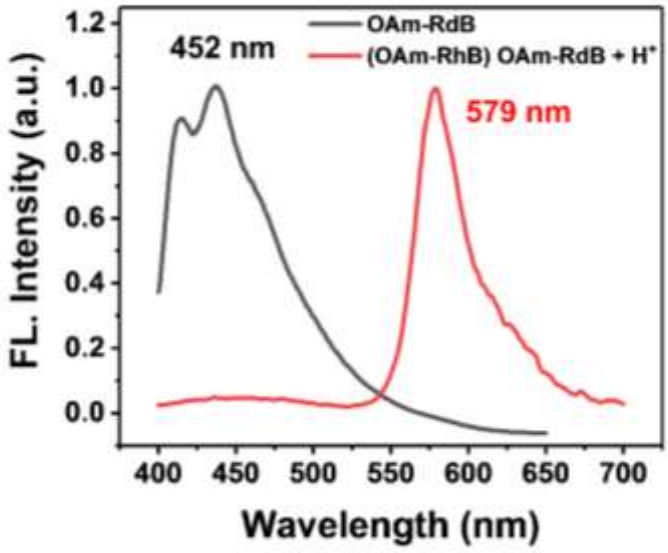

Figure S4. The change in the fluorescence emission spectrum of OAm-RdB after solvothermal reaction under 365 nm excited.

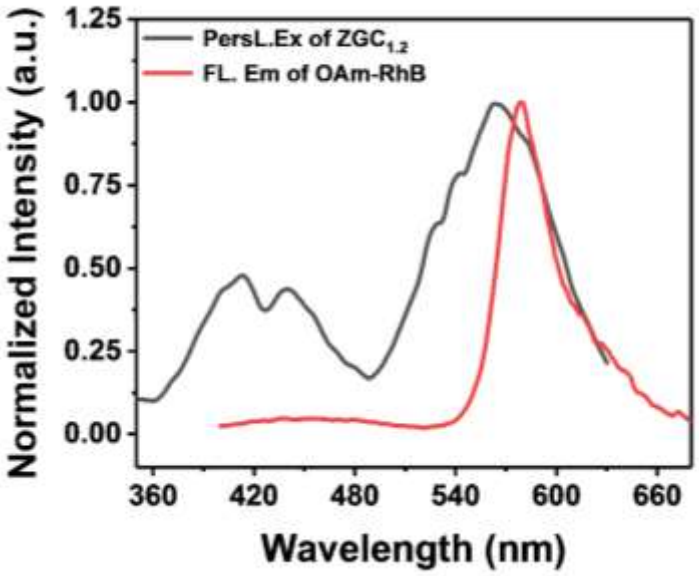

Figure S5. Overlap of the fluorescence emission spectrum of OAm-RhB and PersL excitation spectrum of $ZGC_{1.2}$ PLNPs.

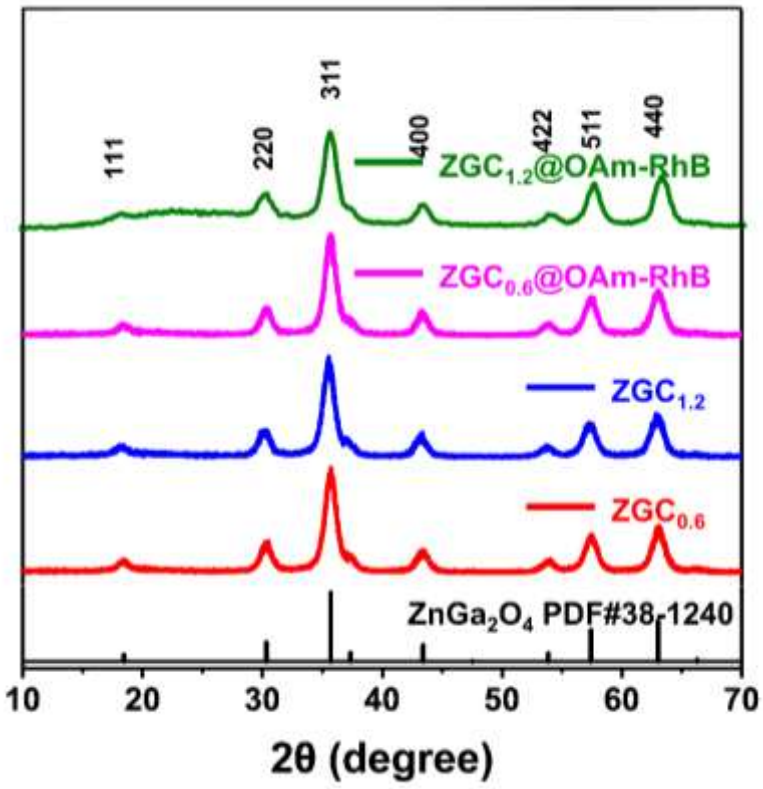

Figure S6. XRD pattern of $ZGC_{0.6/1.2}$@OAm-RhB PLNPs plotted with the standard pattern of cubic spinel phase $ZnGa_2O_4$ (JCPDS No. 38−1240).

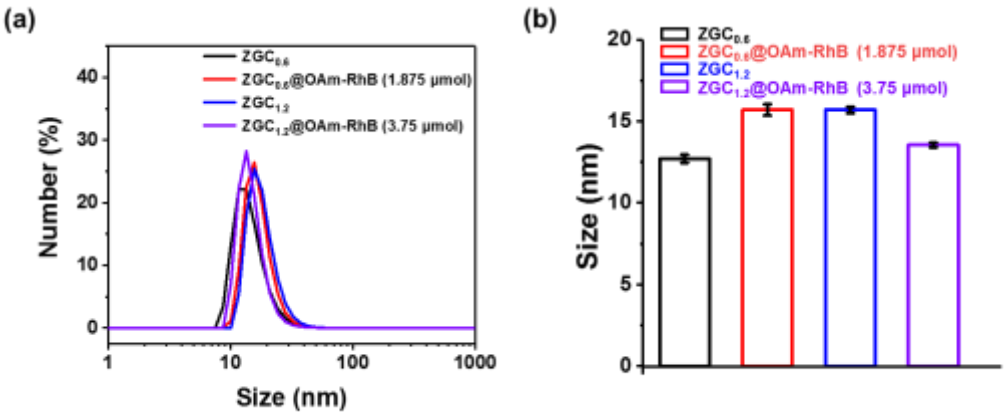

Figure S7. DLS data (a) and statistics analysis (b) of the $ZGC_{0.6/1.2}$@OAm-RhB PLNPs. Values were expressed as the mean ± SD (n = 3).

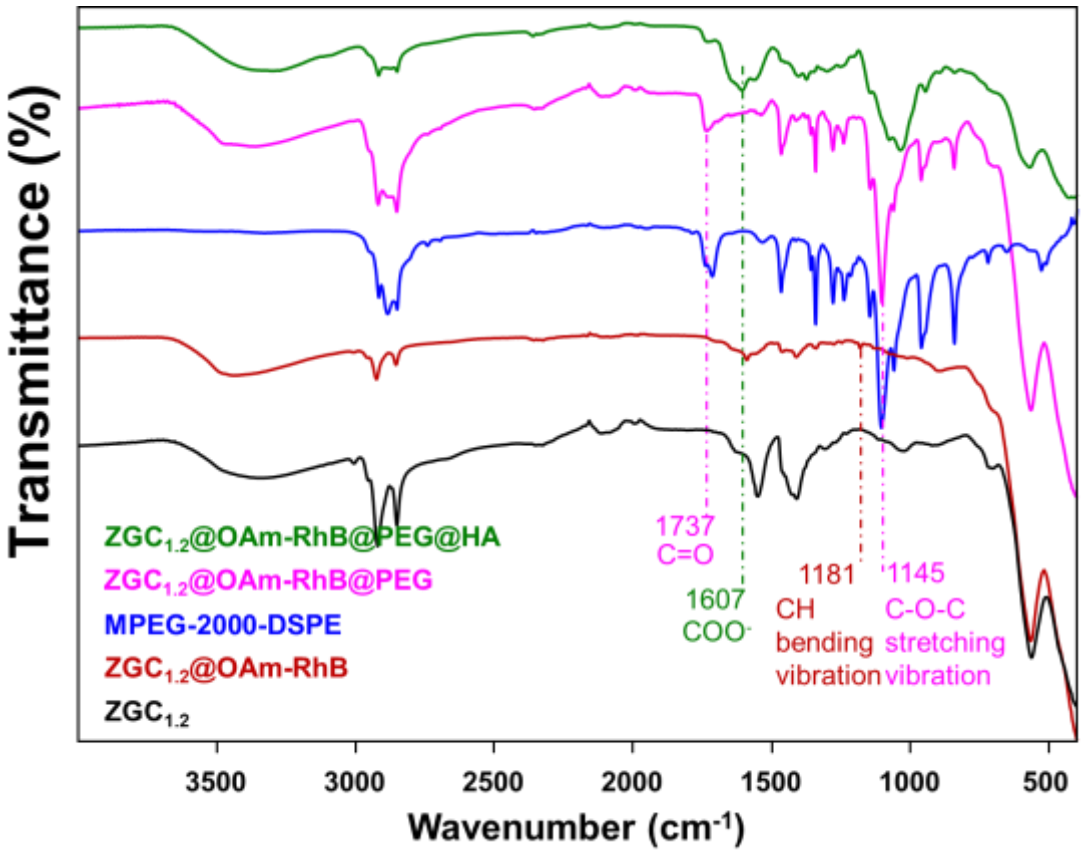

Figure S8. FT-IR spectra of $ZGC_{1.2}$ PLNPs, $ZGC_{1.2}$@OAm-RhB PLNPs, $ZGC_{1.2}$@OAm-RhB@PEG PLNPs, $MPEG_{2000}$-DSPE, and $ZGC_{1.2}$@OAm-RhB@PEG@HA PLNPs.

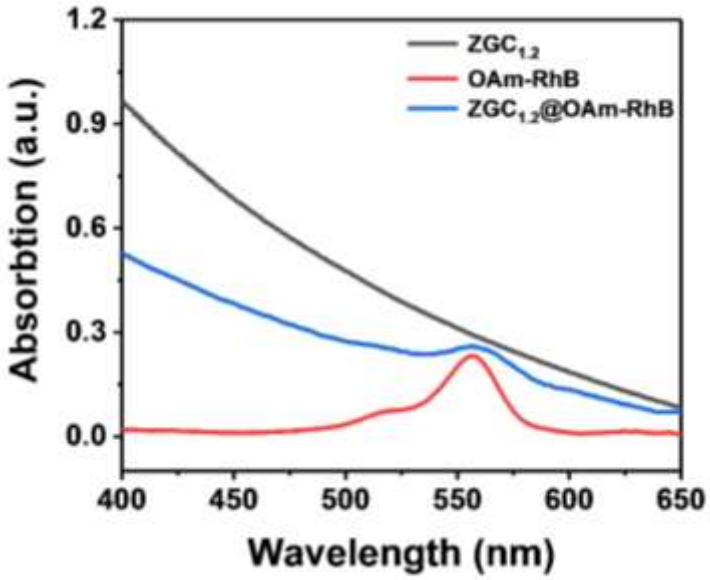

Figure S9. UV-Vis spectra of $ZGC_{1.2}$, OAm-RhB and $ZGC_{1.2}$@OAm-RhB PLNPs.

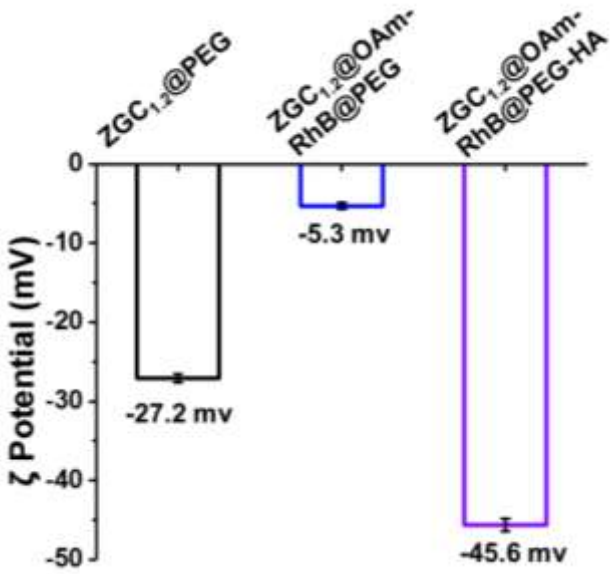

Figure S10. Zeta potential of $ZGC_{1.2}$@PEG, $ZGC_{1.2}$@OAm-RhB@PEG, and $ZGC_{1.2}$@OAm-RhB@PEG@HA.

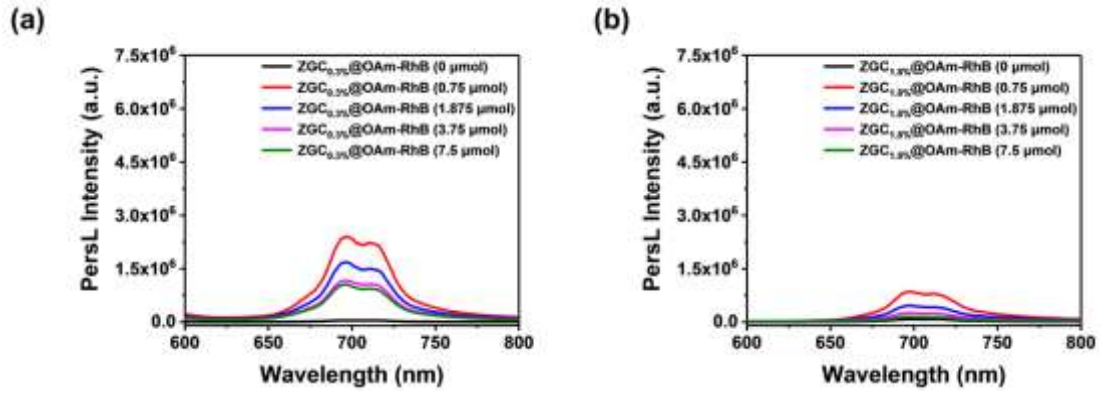

Figure S11. Phosphorescence emission spectra of different amounts of OAm-RhB loaded on (a) $ZGC_{0.3}$ PLNPs and (b) $ZGC_{1.8}$ PLNPs.

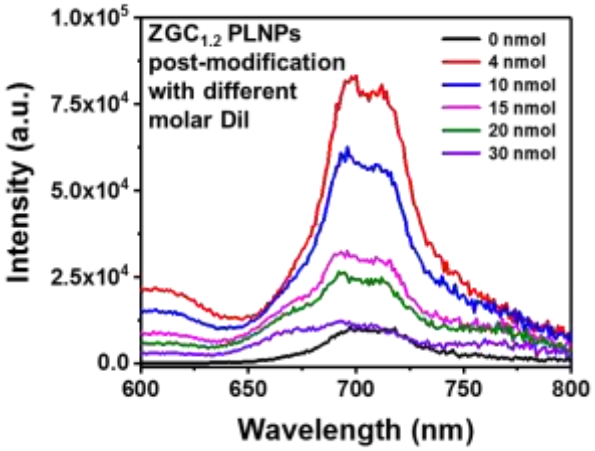

Figure S12. Phosphorescence emission spectra of different amounts of DiI loaded on $ZGC_{1.2}$ PLNPs.

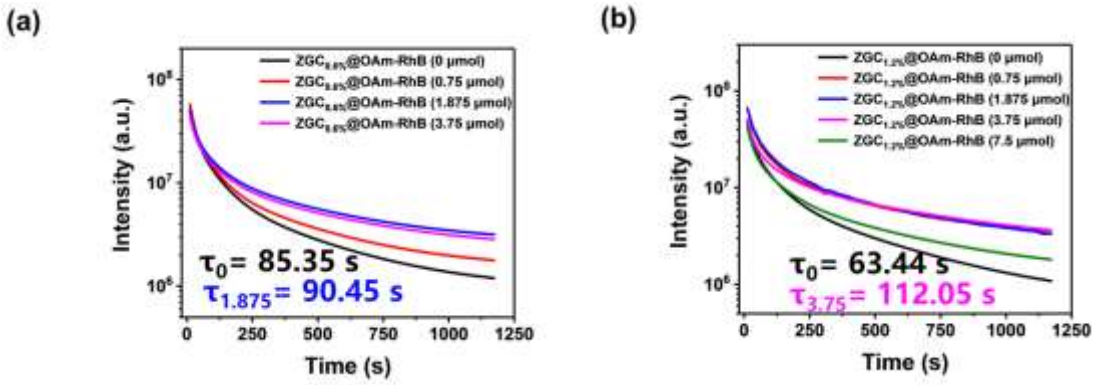

Figure S13. Afterglow decay curve of different amounts of OAm-RhB loaded on (a) $ZGC_{0.6}$ PLNPs and (b) $ZGC_{1.2}$ PLNPs.

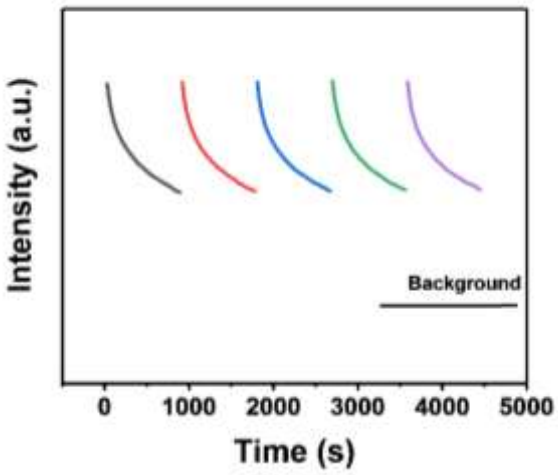

Figure S14. Photostability assessment of $ZGC_{1.2}$@OAm-RhB PLNPs after white LED light recharging.

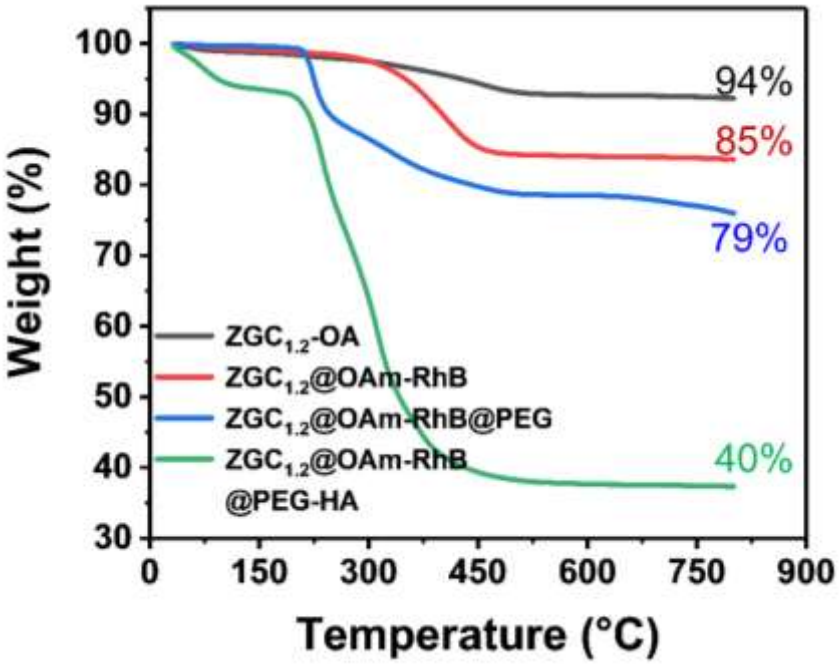

Figure S15. Thermogravimetric analysis of $ZGC_{1.2}$, $ZGC_{1.2}$@OAm-RhB, $ZGC_{1.2}$@OAm-RhB@PEG, and $ZGC_{1.2}$@OAm-RhB@PEG@HA PLNPs.

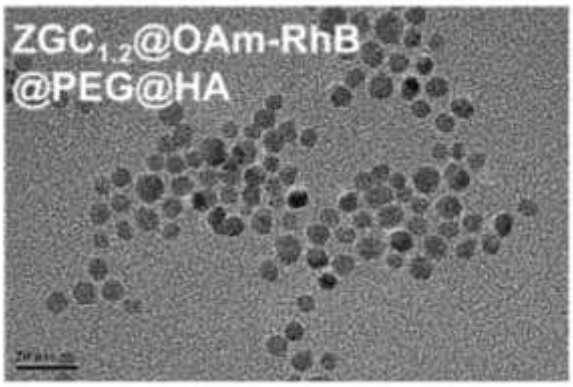

Figure S16. The TEM image of $ZGC_{1.2}$@OAm-RhB@PEG@HA PLNPs. scale bar: 20 nm.

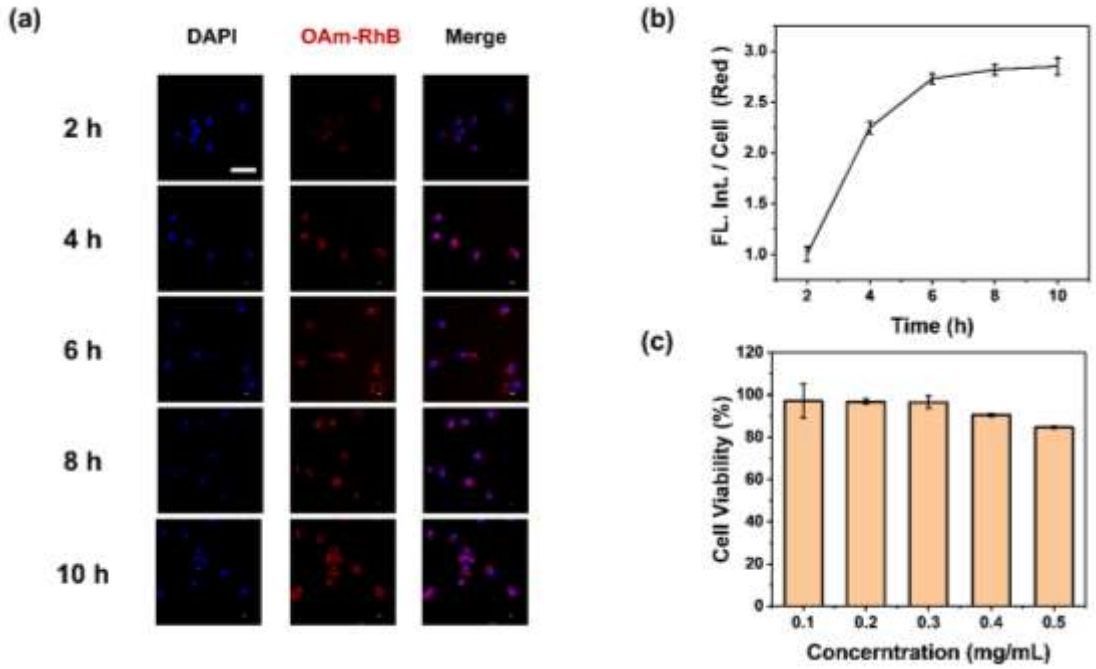

Figure S17. Cellular uptake and cytotoxicity analysis of $ZGC_{1.2}$@OAm-RhB@PEG@HA PLNPs. (a) Confocal laser-scanning microscopic photograph (scale bar = 50 μm). (b) Quantification of red fluorescence per cell of (a) in different time points. (c) Relative growth rate of HepG2 cells after incubation with $ZGC_{1.2}$@OAm-RhB@PEG@HA PLNPs for 48 h. Values were expressed as the mean ± SD (n = 3).

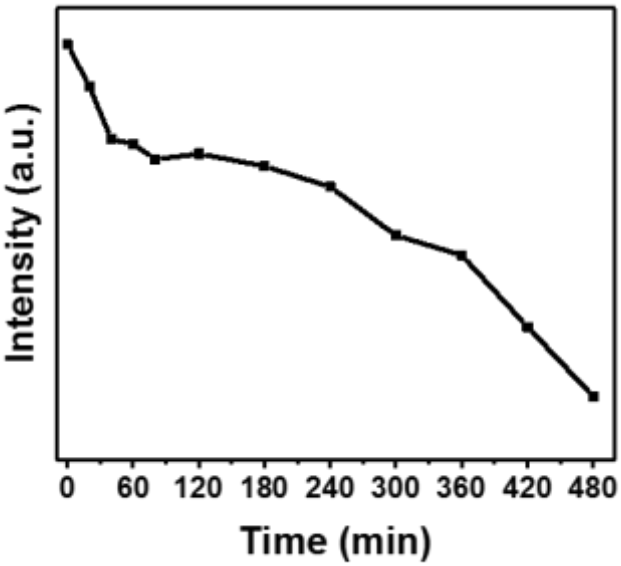

Figure S18. The quantification of luminescence intensity (Figure 6 a) of tumor region in different time point.

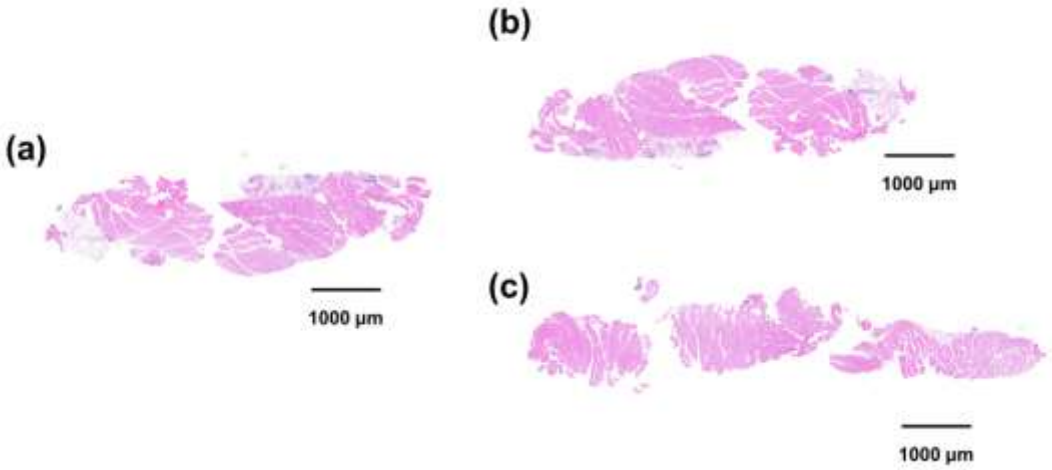

Figure S19. H&E staining of normal tissue near the tumor site.

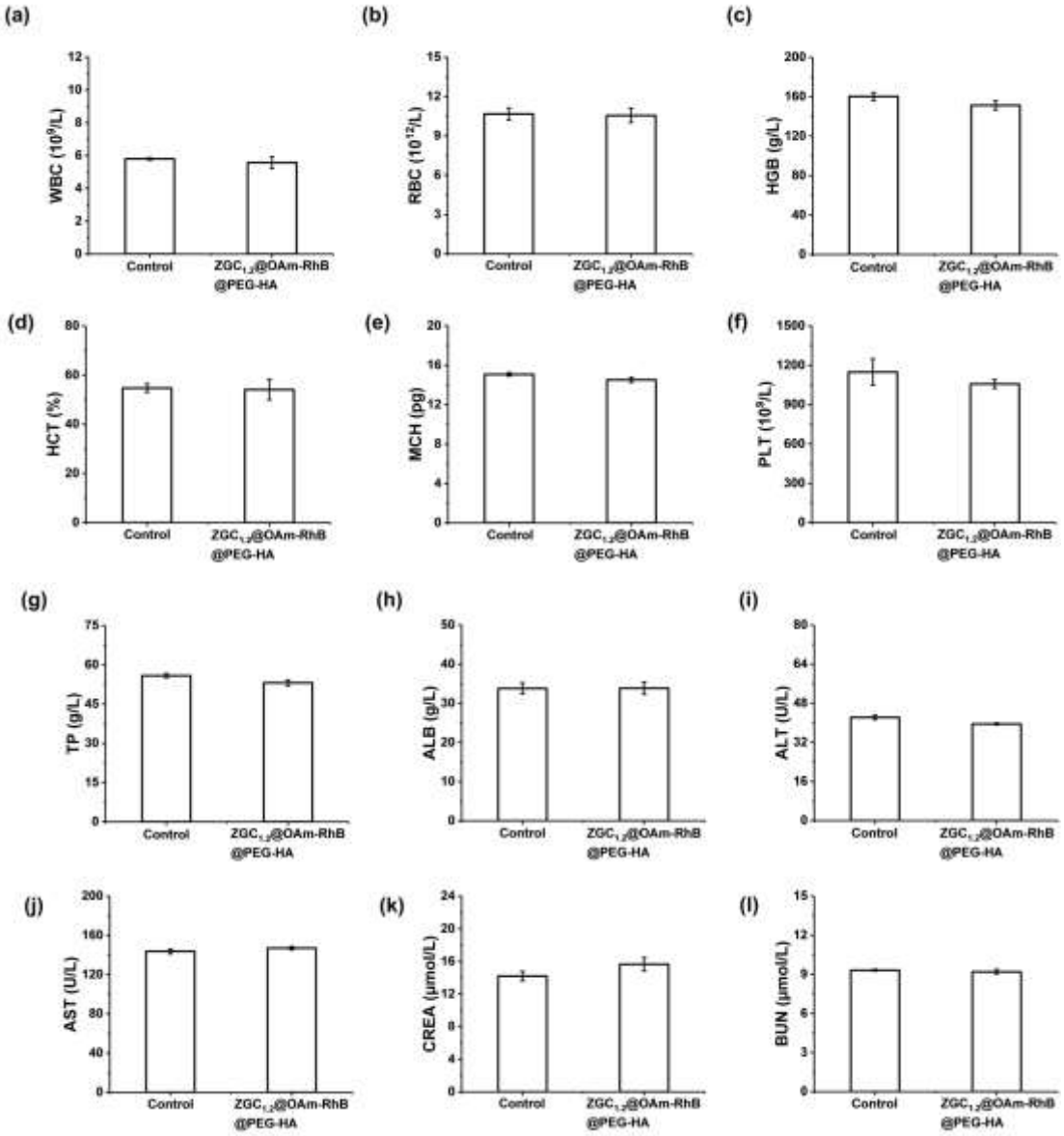

Figure S20. Blood biochemistry and hematology analyses data of healthy mice on day 14 post-injection of normal saline (control) or $ZGCP_{0.5}$-Dil PLNPs. a) white blood cells (WBC), b) red blood cells (RBC), c) hemoglobin (HGB), d) hematocrit (HCT), e) mean corpuscular hemoglobin (MCH), f) blood platelet (PLT), g) total protein (TP), h) albumin (ALB), i) Alanine aminotransferase (ALT), j) aspartate aminotransferase (AST), k) creatinine (CREA), l) blood urea nitrogen (BUN).

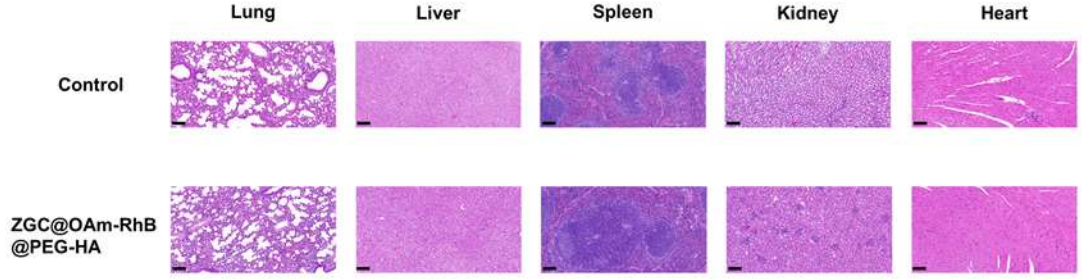

Figure S21. H&E staining of major organs from mice treated with normal saline (control) or $ZGC_{1.2}$@OAm-RhB@PEG@HA PLNPs (Bar = 100 μm).

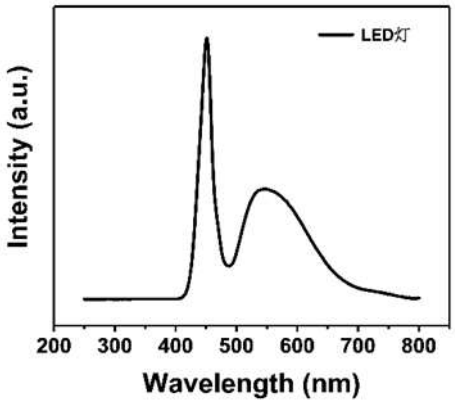

Figure S22. Emission spectrum of excitation light source applied in both in vitro and in vivo experiments.